Characterising the Southern Ocean and Ross Sea wave climate

Sally Garrett [1] Tom Durrant[2]

[1] Defence Technology Agency, New Zealand Defence Force
[2] Oceanum Limited

ABSTRACT

The waves of the Southern Ocean and the Ross Sea are largely unstudied. The New Zealand Defence Force (NZDF) routinely operates in these areas and is currently engaged in a shipbuilding programme which requires a detailed understanding of the wave climate for sea keeping analysis and ice belt design. Unlike other areas, the Southern Ocean and the Ross Sea has limited ship traffic and therefore limited wave observations from volunteer observing ships. Moreover, due to the difficult conditions and remote location limited scientific measurements of waves have been completed. In 2017, the NZDF deployed the first wave buoy in the open ocean south of 47 S anywhere in the world. In addition, 21 free floating buoys were also deployed between 42 S and 67 S. This array has provided an understanding of wave characteristics across the Southern Ocean and the Ross Sea.

The data from these platforms have been used to optimise the WaveWatch III wave forecast model. The optimised setup is then used to create a 24-year hind-cast wave atlas for the ice-free areas south of 31 S.

In this paper, this previously unpublished wave atlas for the Southern Ocean and Ross Sea will be presented. A limited comparison will also be made between the wave statistics from both wave buoys observations and the wave atlas in these regions with the bivariate frequency wave height-period occurrence tables recommended for the North Atlantic by the International Association of Class Societies (International Association of Classification Societies, 2001).

INTRODUCTION

The New Zealand Defence Force (NZDF) routinely operates in Southern Ocean and Ross Sea and is engaged in a shipbuilding programme which requires a detailed understanding of the wave climate for sea keeping analysis and ice belt design. This characterisation of the Southern Ocean and Ross Sea waves is required for all sea areas from 31 S to 78 S year round.

Knowledge of the wave climate of an area is a critical element for the design of vessels and offshore structures. Several studies have attempted to quantify the effect on design of uncertainties caused by a lack of knowledge in the wave climate (Bitner-Gregersen & Guedes Soares, 2007) and have found differences in long-term ship responses of up to 150 % of a

nominal value, e.g. Guedes Soares & Travoa, (1991). This high uncertainty may lead to overdesign/under design of ships, with significant economic and risk-related consequences.

The need to improve the availability, quality and reliability of wave databases has been identified by several professional organisations (Bitner-Gregersen et al., 2009). In addition, the evolution of design processes has increased the detail required of not only the characteristic wave statistics and bivariate frequency wave height-period occurrence tables (scatter diagrams), but also of the full directional wave spectrum (Cardone et al., 2015).

Scatter diagrams based on the historical visual observations of sea state by merchant vessels participating in the Voluntary Observing Ships (VOS) form the basis of the Global Wave Statistics (GWS) atlas (BMT Group, 1986). Products derived from the GWS atlas include the International Association of Class Society recommended wave data (International Association of Classification Societies, 2001). The atlas divides the globe in 104 regions, as illustrated in Figure 1, each with a scatter diagram of historical observations. This data is still employed for ship motion and design studies. However, while this database has been used for many years its accuracy has been questioned by researchers, especially concerning wave period and steepness (Bitner-Gregersen & Guedes Soares, 2007).

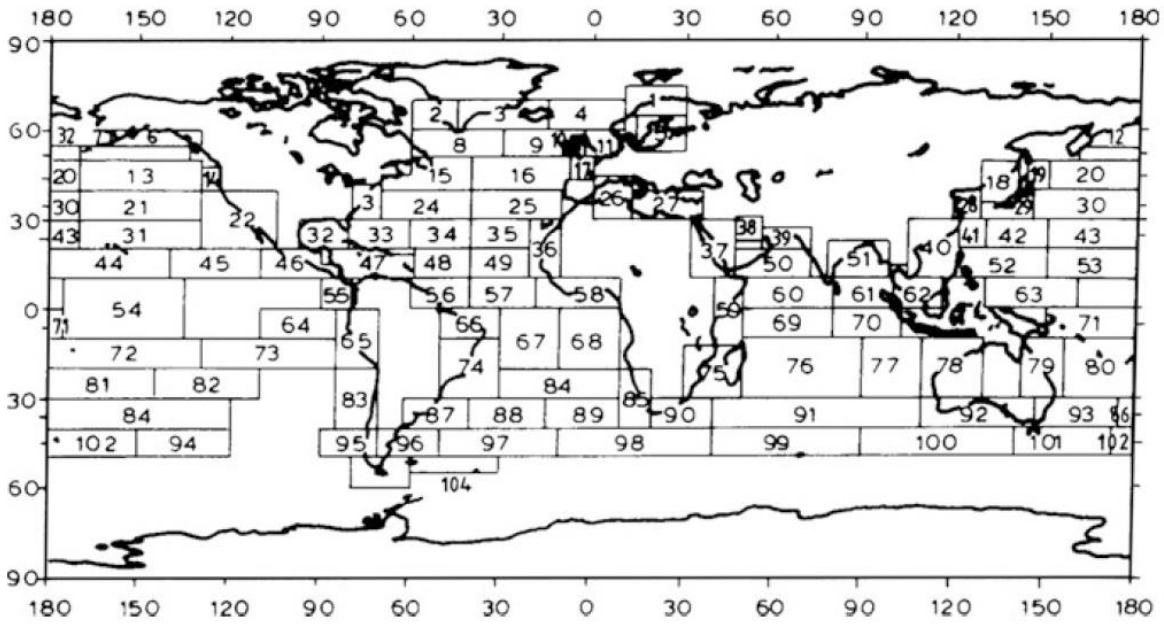

Figure 1 Map of the GWS sea areas. Source:(BMT Group, 1986)

Another shortcoming of the GWS atlas is that is does not have global coverage and does not define the wave climate for the Southern Ocean area. The southernmost latitude of the available GWS data is 50 S (except for the Drake Passage sea area -104); well short of the 77 S ships are able to navigate to in the summer. Professional practise currently recommends the use of a refined GWS scatter diagram for the entire North Atlantic to be used for designing ships operating globally including those operating in the Southern Ocean (International Association of Classification Societies, 2001).

To test if this practise adequately describe the conditions of the Southern Ocean, Cannon, Guzsvany, & Turner (2004) compared the ship motion modelled for an ANZAC-class frigate ship for both the Southern Indian Ocean (GWS sea areas 91, 92, 99, 100, 101) and North Atlantic (GWS sea areas 3, 4, 8, 9). Southern Indian Ocean data from 30 S – 50 S was used due to the absence of data in the Southern Ocean. Overall the global bending moment of a frigate operating in the Southern Indian Ocean was 10% greater than for the same vessel in the North Atlantic.

Slamming calculations were made for a frigate travelling at 7.5 knots in all sea states for head seas only. The number of slams for the same length of simulation was 1.5-3 times greater for the Southern Indian Ocean sea areas compared to the North Atlantic sea areas. The greatest number of slams was modelled for Southern Indian Ocean sea area 100. The pressure of these slams was also modelled, with sea area 100 having the greatest slamming pressures and the average Southern Indian Ocean slamming pressure being 1.2 times higher than when operating in the North Atlantic.

A limitation of this study that was identified was the lack of winter Southern Indian Ocean data due to a lack of shipping in the area, making the results a conservative estimate. However, even considering this limitation the larger global bending moment estimated for the Southern Hemisphere brought doubt to the assumption that North Atlantic sea areas expose ships to the worst sea conditions.

Moreover, a comparison of the GWS data with available satellite altimeter data showed that the Southern Indian Ocean sea areas had a greater peak significant wave height than any area described in the GWS database. While for North Atlantic sea areas the peak significant wave height was similar for GWS and satellite databases, highlighting the GWS data for the Southern Indian Ocean was underestimating the conditions that would be experienced at sea.

At the time of the study wave period data was unable to be collected by satellite and therefore no comparison between satellite wave period and the GWS datasets was made. The inability to accurately sense wave period from space continues today. Synthetic aperture radar (SAR) is the only direct source of wave period estimates available from space. High errors have been identified in this data due to the SAR only capturing the long-wave part of ocean wave fields. Violante-Carvalho (2005) noted that the high-frequency cut-off is sea state dependent but, in general, waves shorter than 10 seconds propagating parallel to the satellite track are not mapped.

The New Zealand Defence Force operates in the Southern Ocean annually. Ship's staff have reported high sea sates on all voyages. This study aims to measure and then model the sea conditions in the Southern Ocean and compare these to the International Association of Classification Societies (2001) scatter diagram for the North Atlantic. This paper provides the initial findings of this new wave characterisation by measurement and modelling, with papers presented by Marsland and Ballard providing details of the implications for ship design.

WAVE CLIMATE MEASUREMENT AND MODELLING

The Southern Ocean is the southernmost part of the global ocean and represents around 22% of the sea surface area. The combination of persistent westerly winds, and the largely unbroken expanse of sea, produces potentially enormous fetches, resulting in the Southern Ocean experiencing higher wave heights for longer periods than any other body of water (Young, 1999). Due to the harsh ocean environment and remote location it is also the least observed of any ocean body.

The NZDF ship building program requires characterisation of the wave conditions year-round in the Southern Ocean and Ross Sea to 78 S. Initial studies of waves in the area to support this aim focussed on three main data sources; ship observations from the Volunteering Observing Ships (VOS) program (Kent et al., 2011), ship motion measurements from Royal New Zealand Navy (RNZN) vessels to enable estimation wave characteristics using the techniques of Nielsen & Stredulinsky (2012) and satellite observations using the Globwav database (Ash et al., 2010). Each of these data sources were unable to provide year-round characteristics for the required spatial extent.

Ship voyages in the Southern Ocean and Ross Sea are currently limited both temporally and spatially (Summerhayes, Dickson, Meredith, Dexter, & Alverson, 2007). Unlike similar latitudes in the Northern Hemisphere ship-based observations both visual and using ship motion sensors in the Southern Ocean currently do not provide year-round wide area coverage of wave conditions.

An example of these spatial and temporal limitations is the cruises completed by the fleet of New Zealand registered ships that operate in the Southern Ocean and Ross Sea routinely. The fleet includes the RNZN Offshore Patrol Vessels, the National Institute of Wave and Atmospheric research (NIWA) research vessel RV TANAGAROA and the fishing vessels conducting toothfish fishing in the Ross Sea. The vessels from each of these groups operate in the Southern Ocean and Ross Sea between November and March, returning to similar areas on each voyage, all routinely make observations. However, no observations are made by the New Zealand Fleet in the winter months and locations where these vessels do not routinely operate.

Tedeschi, Rizzo, & Carrera (2001) study of the route between New Zealand and Terra Nova Bay in the Ross Sea highlights the low number of observations in the winter months. Only 88 observations south of 60 S exist between 160 E and 180 E for wind speed or wave height or wave period summed across the period of April to September for all years from 1960 -2000. For the same 40-year period and longitudes, 5778 observations were made between 50 S and 60 S.

These very low numbers of observations have been associated with high sampling biases (between ship based measurements and models) in the Southern Ocean, where wave height may be underestimated by the VOS fleet by as much as 1–1.5 m because of poor sampling, primarily associated with a fair weather bias of ship routing and observation (Gulev, Grigorieva, Sterl, & Woolf, 2003) . Ship based observations were therefore deemed unsuitable as a sole source of data for developing a ship building wave climatology.

Satellite observations in open water provide a year-round unbiased method of characterising wave height. However altimeters, the most common sensor used, cannot estimate wave height in the presence of sea ice or other non-Gaussian surfaces within the sensor footprint (Ardhuin et al., 2019). For SAR collected images ocean waves are clearly visible in the imagery of ice-covered waters, however their quantitative analysis is presently limited to the estimation of a dominant wavelength and direction (Liu, Holt, & Vachon, 1991; Schulz-Stellenfleth & Lehner, 2002) for wave periods less than 10 seconds (Violante-Carvalho 2005). As this study required wave characteristics within areas with sea-ice coverage, and requires detailed understanding wave period, these limitations meant the use of satellite data was limited to open-water areas for the validation of the wave model outputs.

To enable a year-round understanding of wave conditions in all locations to 78 S a three-part approach was used: in-situ measurement of waves were completed using wave buoys; the data from these buoys along with satellite altimeter measuements was then used to validate a Southern Ocean and Ross Sea optimised setup of the WaveWatch III wave model; this model was then used to create a 24-year hindcast for the area.

The first long-term wave buoy deployment was Southern Ocean Flux Station (SOFS), established as part of the Southern Ocean Time Series project (Trull et al., 2010). Five deployments have been performed since March 2010, providing measurements of wave characteristics and spectra spanning a period of over 700 days. The approximate coordinates of the mooring location were 47 S and 142 E. SFOS was the southernmost directional measurement of waves in the South Pacific sector of the Southern Ocean.

To enable measurements of waves throughout the South Pacific sector of the Southern Ocean an array of free floating and moored wave buoys was deployed from 53 S to 67 S. A combination of free floating and moored wave buoys were used due to the cost and difficulties associated with the deployment of moored wave buoys.

Wave buoys provide point measurements of waves for a short time period. The second part of this study was to hind-cast the wave conditions of the Southern Ocean for a 24 year period. The model outputs were then validated against both the collected wave buoy data and intercalibrated altimeter data.

Observation - Wave Buoy Array

Moored and free-floating wave buoys were used to measure waves from 42 S to 67 S between February 2017 and present. A time series of the latitude of the deployed buoys is shown in Figure 2.

The wave buoy array consisted of the following buoys:

- Two TRIAXS Directional Wave Buoys, the first of which was deployed 11 nm miles south of Campbell Island (52°45.71'S, 169°02.54'E) in February 2017. This buoy broke free in July 2017and was replaced by the present buoy in March 2018.

- Nineteen Miniature Wave Buoys, developed by Scripps Institution of Oceanography (SIO) (Coastal Observing Reserach and Development Center, 2016), deployed from

Royal New Zealand Navy ships and the RV TANGAROA across the Southern Ocean and in the Ross Sea.

- Four Spoondrift buoys deployed in the Southern Ocean from RV TANGAROA during the 2018 Ross Sea cruise.

The moored TRIAXYS buoys were deployed within New Zealand territorial seas, with the location decided upon due to the relatively shallow water depth (~140m) in an area with limited other sea bed features that would cause shoaling of waves.

The latitude of the free-floating buoys was able to be planned with the deploying ships, however the longitude of deployment was decided by the ship.

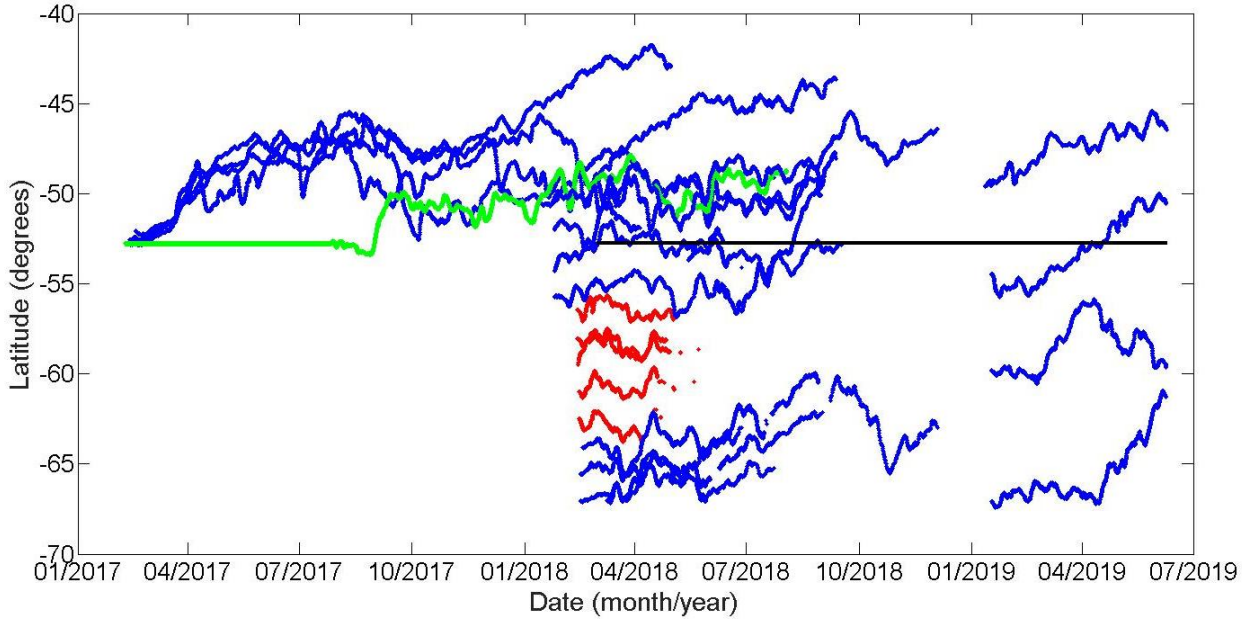

Figure 2 Time series of the latitudes of wave measurements made by SCRIPPS (blue), Spoondrift (red), TRIAXYS 2017 (green) and TRIAXYS 2018 (black) wave buoy deployments

Wave measurements for all buoys were completed using a standard ocean wave measuring regime of sampling at 2 Hz for a sampling burst of 20 minutes. For the TRIAYXS and Spoondrift buoys these sampling bursts occur 3-hourly with hourly sampling for all the SIO buoys. Onboard processing is then completed and wave characteristics including significant wave height, wave peak period, wave peak direction as well as directional spectra are telemetered to shore by satellite.

The TRIAXYS and Spoondrift buoys measure waves using accelerometers (Raghukumar et al., 2017) while the SIO buoys measure waves using GPS (Coastal Observing Reserach and Development Center, 2016).

The data collected from the TIAXYS and Spoondrift buoys are available from https://www.metocean.co.nz/southern-ocean .

Modelling - Southern Ocean Wave Atlas

In order to enable a greater spatial and temporal characterisation of waves a 24 year hind-cast was completed for all ice-free areas south of 31 S. This hind-cast was modelled using the WaveWatch III version 5.16 (Tolman, 1991). The details of the setup of the model is detailed in Southern Ocean Wave Atlas report (MetOcean Solutions Limited, 2019) and summarised in Table 1.

Table 1 Setup parameters for WaveWatch III Southern Ocean hind-cast.

Parameter	Hind-cast setup
Resolution	0.25 deg x 0.2 deg
Extent	31 S – 77.5 S
Period	January 1993 – December 2017
Wind field	ERA5 reanalysis from the European Centre for Medium-Range Weather Forecasts
Current input	GLORYS reanalysis from Mercato Ocean European Copernicus Marine Environment Monitoring Service

The validation of the wave hind-cast was based on intercalibrated altimeter data from 1993 to 2016 from the Globwav multi-altimeter dataset (Ash et al., 2010). The average bias in wave height was less than 0.05 m with a slight overestimation of the smallest waves and a slight underestimation of the largest waves. The root-mean-square deviation was also relatively low with overall values of ~ 0.4 m. Regions covered by ice during part the year had the largest errors, including the coastal areas near Antarctica between 60 E and 120 E and between 180 E and 240 E.

Seasonal bias was calculated for the 1993-2016 period. These biases were generally positive, especially south of 50 S. The largest positive bias was found in the summer season from December to February, with values ~0.2 m throughout the domain and up to 0.4 m in some areas. During the March to May there was a smaller positive bias around 0.15 m on average, with less areas of higher bias compared to summer months. Winter (June to August) had the smallest bias on average, with few regions showing positive bias around 0.05 m, but with surprisingly high negative bias in the ice marginal zone. Spring biases were like those in the March to May period.

Full details of the validation are provided in the Southern Ocean Wave Atlas report (MetOcean Solutions Limited, 2019) and, as this hindcast was only recently completed (June 2019). further analysis will be presented in a series of forthcoming papers.

The data from the 24-year hindcast is available from https://metoceanview.com/ .

The GWS atlas divides the area covered by the atlas into 104 sea areas. These sea areas as shown in Figure 1 are rectangular in shape and in some cases cover locations where bivariate

frequency wave height-period occurrence may have different distributions. For example, area 104 covers both the western and eastern approaches to Cape Horn.

The intent for the newly developed wave atlas was to divide the hind-cast modelled area in to a series of regions with a similar distribution of wave heights and periods. This was completed by calculating the mean significant wave height, the standard deviation of the significant wave height, the mean wave period and the standard deviation of the wave period for each of the 300 months in the hind-cast and then clustering using a K-means algorithm to find areas of similar wave characteristics (MetOcean Solutions Limited, 2019).

The resulting clustering is shown in Figure 3. To increase the usability of the data the grid was divided in to 5 degree x 5 degree regions and the cluster for each region applied from the K-means analysis as shown in Figure 4.

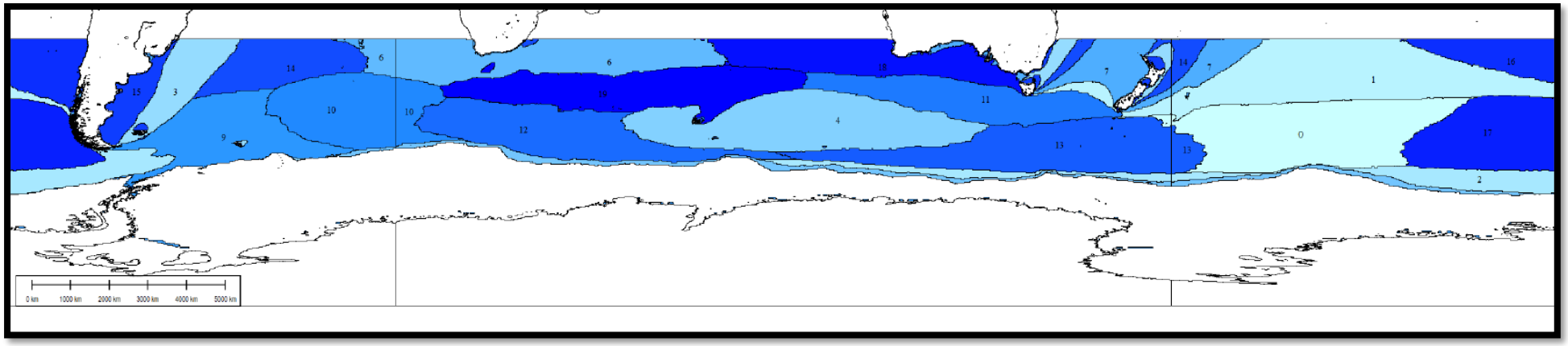

Figure 3 Classification of Southern Ocean zones obtained from K-means clustering

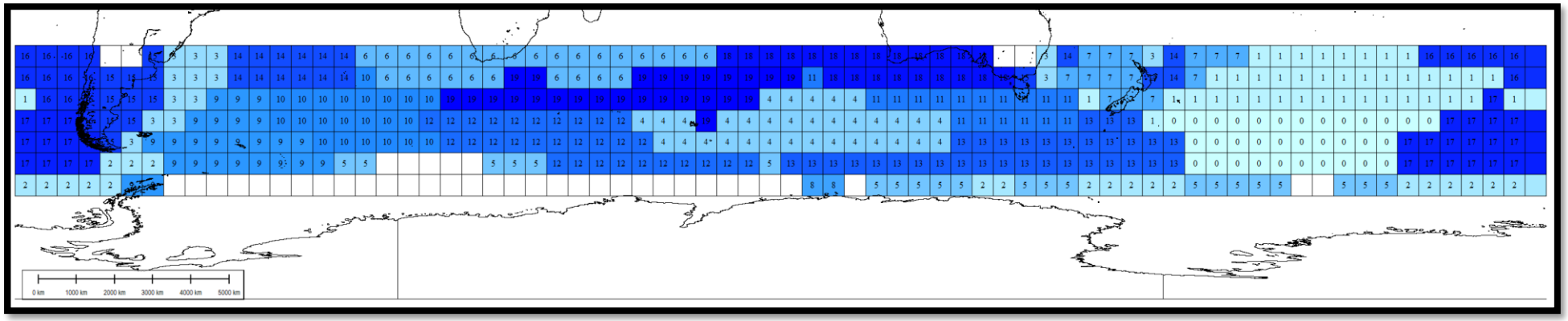

Figure 4 Simplified classification of Southern Ocean zones.

SOUTHERN OCEAN AND ROSS SEA WAVE CLIMATE

Wave Measurements

In total 5622 buoy days (at June 1st 2019) of wave data has been collected at latitudes between 42 S and 67 S in the South Pacific sector of the Southern Ocean. The only buoy to have collected data for a 12-month period south of 50 S (the area outside the GWS sea areas) is the TRIAXYS buoy deployed in March 2018. This dataset will be used for the comparison against the IACS North Atlantic data.

In the Ross Sea only free floating buoys were deployed. The longest wave buoy record south of 60 S is currently 142 days in duration; after this time the buoy drifted into the Southern Ocean. 30-day records from each of four wave buoys were used in addition to the 142 day time series to develop an understanding of waves in the area.

Figure 5 shows the occurrence of significant wave heights for each of the three regions. For measured wave data in both the Southern Ocean and the Ross Sea the largest number of observations was between 4-5m. For the IACS North Atlantic data this peak is for waves with a significant wave height between 3–4m. However, the occurrence of higher sea states in the IACS table was greater than the Ross Sea observations for all wave heights greater than 5m and greater than the Campbell Island buoy for all wave heights greater than 7m.

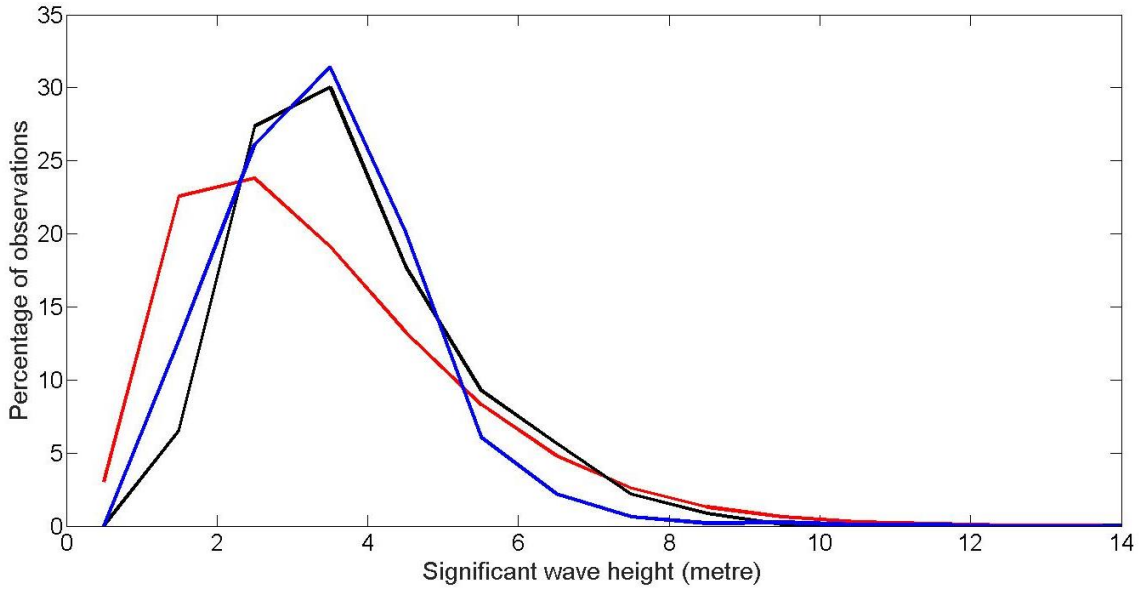

Figure 5 Distribution of significant wave heights for International Association of Class Society North Atlantic sea area (red), Campbell Island TRIAXYS wave buoy (black) and Ross Sea SCRIPPS wave buoys (blue).

Figure 6 shows the occurrence of peak wave period for each of the three regions. Wave period was greater for the observational datasets, with the Ross Sea data having the greatest peak wave period. The Ross Sea dataset was collected with free floating GPS buoys, however the ability of these buoys to measure long period waves has not been extensively researched and it is possible the variations between the two observed datasets is associated with sensor limitations. The Campbell Island wave buoy has a peak at 8.5 seconds, further analysis is

required to determine the reason for this peak, however the majority of the waves at the period come from a North West direction where the fetch is affected by Campbell Island.

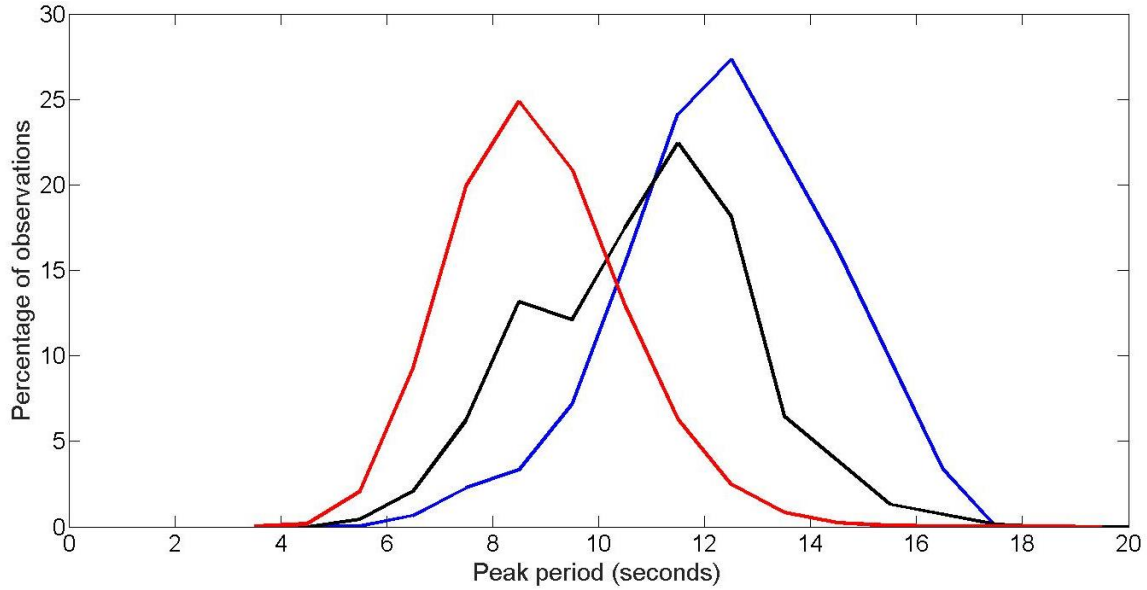

Figure 6 Distribution of peak period for International Association of Class Society North Atlantic sea area (red), Campbell Island TRIAXYS wave buoy (black) and Ross Sea SCRIPPS wave buoys (blue).

The IACS table's largest wave heights were between 16-17m with periods between 10-16 seconds. For the Campbell Island observation, they were 15-16m at 16-17 seconds and for the Ross Sea the largest wave height was between 12-13m. However, as the wave buoys are a point measurement of waves and the length of each observational time series is short, it is difficult to compare these maximum values to the long-term time series of the IACS data. For this reason, the hind-cast was completed.

Wave Atlas

Wave height distributions for the 20 zones of the Southern Ocean Wave Atlas (SOWA) compared to the IACS North Atlantic dataset are shown in Figure 7. The significant wave height distributions for the SOWA zones vary in terms of peak significant wave height and also in distribution of wave height greater than 6m. 12 of the SOWA zones have a peak significant wave height greater than the peak of between 3-4m of the IACS. Moreover, 8 zones have a higher proportion of waves greater than 6m than the IACS, and 2 zones have a higher proportion of waves greater than 8m.

At high sea states the largest wave heights for the 20 zones is between 15-16m, while for the IACS data it is between 18-19m. However, only 0.00198% in the IACS data set are greater than 16m. Additional understanding is required of the distribution of extreme sea states in the Southern Ocean, in particular whether the SOWA zones should include calculated wave height extremes or remain only distributions of significant wave height.

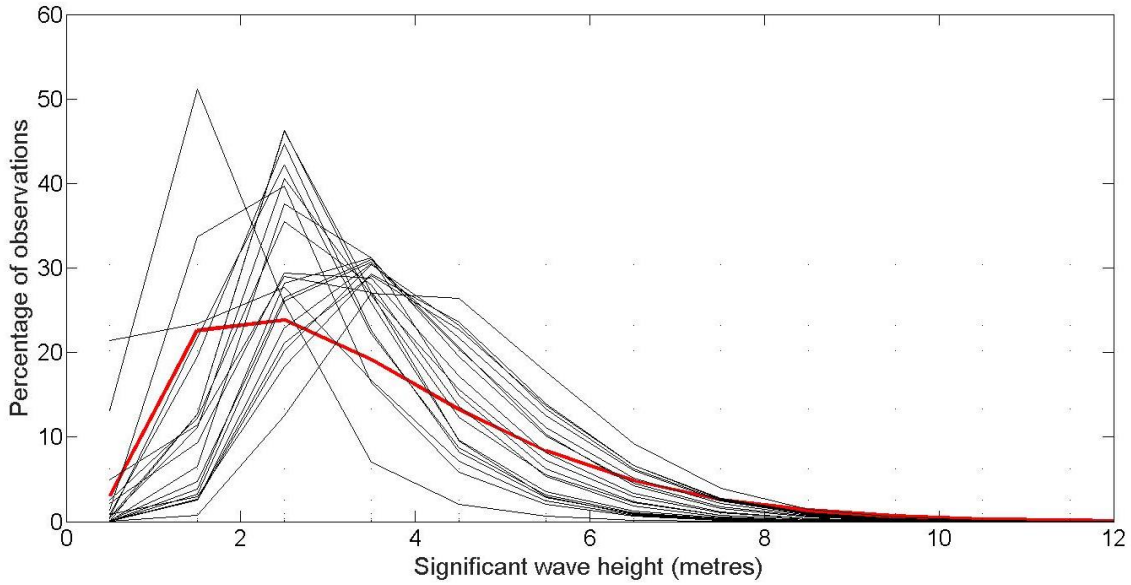

Figure 7 Distribution of significant wave heights for International Association of Class Society North Atlantic sea area (red), wave hind-cast zones 0-19 (black)

Wave peak period distributions for the 20 zones of the SOWA compared to the IACS North Atlantic dataset are shown in Figure 8. For 18 of the 20 SOWA sea areas the peak of the peak period distribution is greater than the IACS with all SOWA sea areas having a greater percentage of wave periods than the IACS for periods greater than 12 seconds. This is consistent with the observational data presented above and also with the work by (Bitner-Gregersen & Guedes Soares, 2007)

A bimodal distribution in wave peak period is shown for SOWA sea area 9 located to the east of the Drake Passage and the Antarctic Peninsula. This sea area also has a large percentage of lower significant wave height in its distribution, indicating the effects of land on the seas in the area.

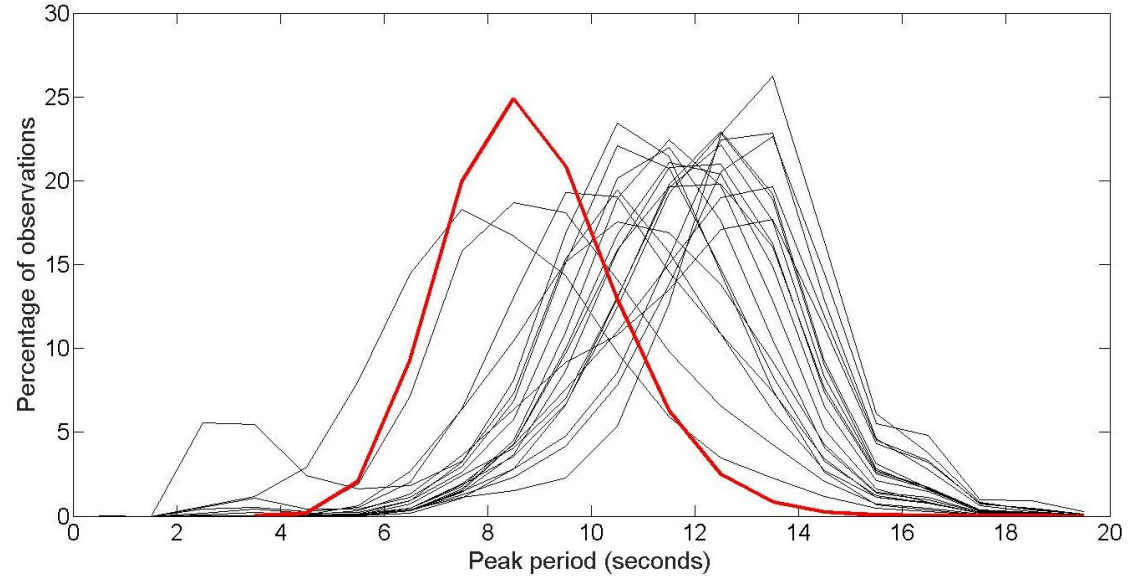

Figure 8 Distribution of peak wave period for International Association of Class Society North Atlantic sea area (red), wave hind-cast zones 0-19 (black)

CONCLUSIONS

In this study a series of short-term wave buoy deployments have been used to characterise the waves across the Southern Ocean south of New Zealand and the northern Ross Sea, to enable comparison to the IACS wave data for the North Atlantic. The aim of this comparison was to gain an understanding of whether the IACS recommendation 34, to use the North Atlantic data for worst case conditions for design, is appropriate for Southern Ocean ships. The observational datasets indicate that the average wave conditions experienced in this area represent greater significant wave heights and longer periods than those specified by IACS. However, higher sea states occur at greater frequency in the IACS tables.

The collected wave data has several limitations including the short length of each deployment and the limited spatial coverage. The TRIAYXS wave buoy data from Campbell Island included 12 months of data, while the Ross Sea collection period was 262 days. Spatially, all buoy deployments occurred in the Southern Ocean Pacific Ocean sector.

To address these limitations a 24 year hind-cast for all ice-free sea areas south of 30 S globally was developed. This data was then divided into sea areas based on similar significant wave height and peak period. As with the observational datasets, the modelled datasets indicate that the average wave conditions experienced in the Southern Ocean have a higher significant wave height and longer period than those specified by IACS. However, they also indicate once again that higher sea states occur at greater frequency in the IACS tables. This is an area for further research.

The findings of this study conclude that bivariate frequency wave height-period occurrence tables for the Southern Ocean and Ross Sea differ from the recommend IACS tables. These differences of a greater average significant wave height and period are the same as that noted from the Southern Indian Ocean by Cannon (2004), who linked the greater average significant wave height and wave period caused a 10% greater global bending moment in an ANZAC frigate.

This programme of work continues with the characterisation of wave spectra using the observations and hind-cast in this paper to compare to industry standard spectra and, if appropriate, the development of specialised spectra for the Southern Ocean.

REFERENCES

Ardhuin, F., Stopa, J. E., Chapron, B., Collard, F., Husson, R., Jensen, R. E., … Young, I. (2019). Observing Sea States. *Frontiers in Marine Science*, *6*, 124. https://doi.org/10.3389/fmars.2019.00124

Ash, E., Busswell, G., (2010). *Amendment History*. Globwave . Retrieved from http://www.globwave.org/content/download/16022/104639/version/1/file/GlobWave_D.7_PUG3_v1.0.pdf

Bitner-Gregersen, E. M., Ellermann, K., Ewans, K. C., Falzarano, J. M., Johnson, M. C., Nielsen, U. D., … Waseda, T. (2009). *17 th INTERNATIONAL SHIP AND OFFSHORE STRUCTURES CONGRESS 16-21*. Retrieved from http://www.issc2018.org/images/issc2009/ENVIRONMENT.pdf

Bitner-Gregersen, E. M., & Guedes Soares, C. (2007). Uncertainty of average wave steepness prediction from global wave databases. *Advancements in Marine Structures - Proceedings of MARSTRUCT 2007, The 1st International Conference on Marine Structures*, (January 2007), 3–10.

BMT Group. (1986). *Global Wave Statistics*. London .

Cannon, S., Guzsvany, G., & Turner, T. (2004). A Study of the Effect of Wave Loading on a Frigate Operating in the Southern Ocean Versus the North Atlantic. In *Proceedings of Pacific 2004 International Maritime Conference* (p. 543). Pacific 2004 International Maritime Conference Managers.

Cardone, V. J., Callahan, B. T., Chen, H., Cox, A. T., Morrone, M. A., & Swail, V. R. (2015). Global distribution and risk to shipping of very extreme sea states (VESS). *International Journal of Climatology*, *35*(1), 69–84. https://doi.org/10.1002/joc.3963

Coastal Observing Reserach and Development Center. (2016). *Miniature Wave Buoy Operating Manual*.

Guedes Soares, C., & Travoa, C. (1991). Influence of wave climate modelling on the long-term prediction of wave induced responses of ship structures. (p. 338). Dynamics of marine vehicles and structures in waves : proceedings of an International Union of Theoretical and Applied Mechanics Memorial Symposium on the Dynamics of Marine Vehicles and Structures in Waves, held at Brunel University, Uxbridge, U.K., 24-2: Elsevier. Retrieved from https://trid.trb.org/view/439995

Gulev, S. K., Grigorieva, V., Sterl, A., & Woolf, D. (2003). Assessment of the reliability of wave observations from voluntary observing ships: Insights from the validation of a global wind wave climatology based on voluntary observing ship data. *Journal of Geophysical Research*, *108*(C7), 3236. https://doi.org/10.1029/2002JC001437

International Association of Classification Societies. (2001). Standard Wave Data (North Atlantic Scatter Diagramm), *34*(34), 1–4.

Kent, E. C., Ball, G., Berry, D. I., Fletcher, J., Hall, A., North, S., & Woodruff, S. D. (2011). THE VOLUNTARY OBSERVING SHIP (VOS) SCHEME. In J. Hall., D. E. Harrison, & D. Stammer (Eds.), *Proceedings of OceanObs'09: Sustained Ocean Observations and Information for Society*.

Liu, A. K., Holt, B., & Vachon, P. W. (1991). Wave propagation in the marginal ice zone: Model predictions and comparisons with buoy and synthetic aperture radar data. *Journal of Geophysical Research*, *96*(C3), 4605. https://doi.org/10.1029/90JC02267

MetOcean Solutions Limited. (2019). *Southern Ocean Wave Atlas*. Raglan, New Zelaland.

Nielsen, U. D., & Stredulinsky, D. C. (2012). Sea state estimation from an advancing ship – A

comparative study using sea trial data. *Applied Ocean Research*, *34*, 33–44. https://doi.org/10.1016/J.APOR.2011.11.001

Raghukumar, K., Chang, G., Spada, F., Jones, C., Gans, W., & Janssen, T. (2017). Wave-Measuring Performance Characteristics of Spoondrift Spotter. *Ocean Waves Workshop*. Retrieved from https://scholarworks.uno.edu/oceanwaves/2017/posters/2

Schulz-Stellenfleth, J., & Lehner, S. (2002). Spaceborne synthetic aperture radar observations of ocean waves traveling into sea ice. https://doi.org/10.1029/2001JC000837

Summerhayes, C., Dickson, B., Meredith, M., Dexter, P., & Alverson, K. (2007). Observing the polar oceans during the International Polar Year and beyond. *World Meteorological Organisation Bulletin* , *54*(4). Retrieved from https://ane4bf-datap1.s3-eu-west-1.amazonaws.com/wmocms/s3fs-public/article_bulletin/related_docs/oceans.pdf?6DGXFFWhtEF5kVJ0lV8ZkeU0if6i.8P8

Tedeschi, R., Rizzo, C., & Carrera, G. (2001). *Weather conditions along the route New Zealand - Terra Nova Bay*. Genova.

Tolman, H. L. (1991). A Third-Generation Model for Wind Waves on Slowly Varying, Unsteady, and Inhomogeneous Depths and Currents. *Journal of Physical Oceanography*, *21*(6), 782–797. https://doi.org/10.1175/1520-0485(1991)021<0782:ATGMFW>2.0.CO;2

Trull, T. W., Schulz, E., Bray, S. G., Pender, L., McLaughlan, D., Tilbrook, B., … Lynch, T. (2010). The Australian Integrated Marine Observing System Southern Ocean Time Series facility. In *OCEANS'10 IEEE SYDNEY* (pp. 1–7). IEEE. https://doi.org/10.1109/OCEANSSYD.2010.5603514

Violante-Carvalho, N. (2005). On the Retrieval of Significant Wave Heights from Spaceborne Synthetic Aperture Radar (ERS-SAR) using the Max-Planck Institut (MPI) Algorithm, *77*(4), 745–755. Retrieved from www.scielo.br/aabc

Young, I. R. (1999). Seasonal variability of the global ocean wind and wave climate. *International Journal of Climatology*, *19*(9), 931–950. https://doi.org/10.1002/(SICI)1097-0088(199907)19:9<931::AID-JOC412>3.0.CO;2-O